Microstructure Effect on the Phase Behavior of Blends of Deuterated Polybutadiene and Protonated Polyisoprene

Richard N. Thudium*

Corporate Research, The Goodyear Tire & Rubber Company, Akron, Ohio 44305

Charles C. Han

Polymers Division, National Institute of Standards and Technology, Gaithersburg, Maryland 20899

Received August 23, 1995; Revised Manuscript Received December 4, 1995[⊗]

ABSTRACT: Small-angle neutron scattering (SANS) was used to measure the miscibility of blends of protonated polyisoprene (HPI) with 3,4 microstructure in the range of 7−44%, and of deuterated polybutadiene (DPB) with 1,2 microstructure in the range of 9−70%. These data suggest that, for deuterated polybutadiene/protonated polyisoprene blends, overall miscibility is controlled by the 3,4 content of the polyisoprene. This isomeric group is strongly immiscible with the 1,4 butadiene group and the immiscibility decreases with temperature, while the 3,4 group is weakly miscible with the 1,4 isoprene group and miscibility increases with temperature. Conversely, the 3,4 group is strongly miscible with the 1,2 butadiene group and miscibility decreases with increasing temperature. The differing trends of the interaction parameter with temperature suggest that shifts in the LCST phase diagram can be controlled by judicious changes in microstructure. These theoretical predications were confirmed with experimental small-angle light scattering (SALS) results on all protonated blends. The statistical segment length, b, appears to be independent of temperature, but is dependent on total vinyl level. For the blends used in this study, b has a minimum value at approximately 30−35% total vinyl isomeric groups.

Introduction

Miscibility of polymer blends is of particular interest in the tire industry because of the effect that miscibility might have on the properties of tire compounds. The polymer characteristics of a binary blend that can affect the blend miscibility are molecular weights, polydispersity, microstructure, and polymer−polymer composition. Small-angle neutron scattering (SANS)[1−7] has been used to study the miscibility of binary polymer blends. The SANS analysis determines the effective polymer−polymer interaction parameter, χ, from the fitting of scattering curves using the scattering theory of de Gennes[8] based on random phase approximation (RPA) for a homogeneous binary blend. Since one of the polymers must be deuterated to provide contrast for SANS, the isotopic effect of deuteration on miscibility has not been fully investigated for diene polymers. Assuming the isotopic effect is negligible to the miscibility, a knowledge of the temperature and compositional effect of χ from SANS analysis can be used along with the polymer characteristics of microstructures, molecular weights, and polydispersity to predict miscibility. Then, rubber blends with desired properties could be designed from computer modeling programs.

Previous papers have shown that the DPB/HPI blend system with a narrow range of microstructures for both polymers has a lower critical solution temperature (LCST) phase morphology using SANS and SALS techniques.[1,2] It was the purpose of this work to investigate the microstructure effects on the miscibility of deuterated polybutadiene/protonated polyisprene (DPB/HPI) blends of a wide range of diene microstructures. It is also the purpose of this paper to evaluate the theory of random copolymer mixtures as reported by ten Brinke, Karasz, and MacKnight[9] and by Paul and Barlow[10] for the DPB/HPI blend system.

[⊗] Abstract published in *Advance ACS Abstracts,* February 15, 1996.

Experimental Section

Protonated polyisoprenes and deuterated polybutadienes were synthesized anionically with *n*-butyllithium and tetramethylethylenediamine modifier to obtain narrow molecular weight distributions and predictable microstructure. One part per hundred Wingstay K was added to each polymer as an antioxidant. The polymer characterization data are given in Table 1. Molecular weights were determined by GPC with six ultrastyragel columns with chloroform as the carrier solvent. Fourteen polystyrene standards ranging from 10 million to 500 molecular weight were used to determine the universal calibration curve. A broad molecular weight polybutadiene internal standard was included in each set of samples. Mark−Houwink constants, derived from measured microstructures, were used to obtain actual molecular weight averages. The microstructural data were determined from 75 MHz ^{13}C NMR spectra. Samples were dissolved in $CDCl_3$ solvent and measured in 10-mm probes for the NMR analysis. The glass transition temperature, T_g, of each sample and polymer−polymer blend was determined by the DSC using a scanning speed of 10 °C/min from −100 to 40 °C.

SANS measurements were made at the Cold Neutron Research Facility at the National Institute of Standards and Technology using experimental methods and data reduction procedures described by Glinka, Rowe, and LaRock.[11] The monochromatized neutron beam was set at a wavelength λ = 9 Å ($\Delta\lambda/\lambda$ = 0.25) on the 8 m SANS unit. The scattering intensity data were collected with a 64 × 64 cm^2 position sensitive counter with 128 × 128 pixels and a sample-to-detector distance of 3.6 m. The intensity data were corrected for sample transmittance, detector noise, and empty sample cell and converted to absolute intensities using a silica gel standard[11] over the scattering angle range ($q = 4\pi \sin\theta/\lambda$, 2θ = scattering angle). The q range of the neutron scattering intensities for this experimental work was 0.004−0.07 Å^{-1}.

Samples for SANS measurements were prepared by casting the DPB/HPI blends from toluene solutions at 30 °C, drying in air, and then drying in vacuum at room temperature for several days before placing in sample holders. Three blends, 30/70, 50/50, and 70/30, were made for each set of DPB/HPI blends for the SANS measurements. All blends were also scanned on the DSC to check for a single T_g, implying miscibility, before making the temperature scan on the SANS

0024-9297/96/2229-2143$12.00/0

Table 1. Characterization Data

Protonated Polyisoprene (HPI)								
					microstructure (%)			
sample	T_g (°C)	$10^{-3}M_n$	$10^{-3}M_w$	M_w/M_n	3,4	cis-1,4	trans-1,4	1,2
HPI-7	−64	32	36	1.13	7	77	16	0
HPI-21	−53	26	28	1.09	21	62	15	2
HPI-44	−34	16	19	1.13	44	33	15	8

Deuterated Polybutadiene (DPB)							
					microstructure (%)		
	T_g (°C)	$10^{-3}M_n$	$10^{-3}M_w$	M_w/M_n	1,2	cis-1,4	trans-1,4
DPB-9	−95	42	45	1.07	9	39	52
DPB-26	−85	40	44	1.08	26	29	45
DPB-39	−79	16	18	1.12	39	24	37
DPB-70	−47	30	37	1.22	70	12	18

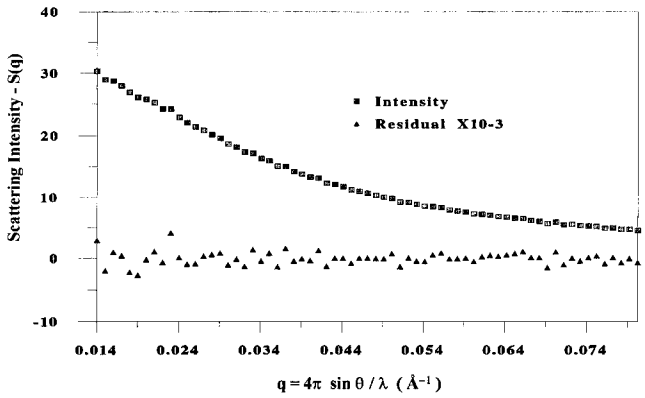

Figure 1. SANS profile of 52/48 blend of 7% 3,4 HPI/70% 1,2 DPB at 35 °C and residuals (difference of experimental and calculated).

unit. Miscibility at room temperature was an essential condition for each blend. All blends were placed between two pure copper foils (0.165 mm thick) with 1.6 mm bushing spacers and locked into holders for SANS experiments. Blends were placed in a vacuum oven before sealing into holders to remove air bubbles. Sample cells were placed in the copper heating block inside the sample chamber of the SANS unit. The temperature was controlled within 0.2 °C and raised stepwise from room temperature to 100 °C to measure the temperature dependence of the neutron scattering profile.

Results and Discussion

The SANS profiles, $S(q)$, at nine different temperatures for each polymer−polymer blend in the single-phase state were analyzed to determine the effective interaction parameter, χ, using random phase approximation (RPA) theory[8] to obtain a best fit. This gave χ as a function of temperature, T. Figure 1 shows one neutron scattering profile at 35 °C and residuals between the experimental and the best fitted theoretical line. From mean field theory, the total structure factor,[4] $S(q)$, is given by:

$$k_N/S(q) = 1/[\phi_A N_A v_A S_D(U_A)] + 1/[\phi_B N_B v_B S_D(U_B)] - 2\chi/v_0 \quad (1)$$

where N_i, ϕ_i, v_i, $S_D(U_i)$, and k_N are degree of polymerization, volume fraction, monomeric molecular volume, Debye's scattering function (single Gaussian chain structure factor), and the contrast factor,[4] which is assumed to be given by

$$k_N = N_0(a_A/v_A - a_B/v_B)^2 \quad (2)$$

with N_0 being Avogadro's number, a_i the scattering length per mole of monomer, and v_0 and v_i the molar volumes of a reference unit cell ($v_0 = (v_A v_B)^{1/2}$) and of the ith segment, respectively. The molar volumes were corrected for thermal expansion from linear expansion coefficients (α) for protonated polymers provided by Walters and Bell.[12] The α and v_i values for the protonated polymers are given in Table 2. The α and v_i values did not change significantly with the range of microstructures used in this work.

Table 2. Expansion Coefficients and Monomeric Molecular Volumes

polymer	$\alpha \times 10^{-4}$ (deg^{-1})	v_i (25 °C) (mol cm^3)
polyisoprene	1.87	74.6
polybutadiene	2.35	60.4

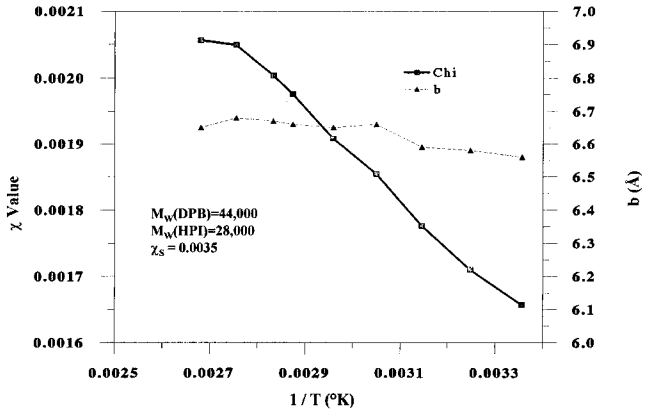

Figure 2. χ and b for 52/48 blend of 21% 3,4 HPI/26% 1,2 DPB versus $1/T$ (K).

The single-chain structure factor, $S_D(U_i)$, is represented by the Debye function:

$$S_D(U_i) = (2/U_i^2)[\exp(-U_i) - 1 + U_i] \quad (3)$$

with $U_i = q^2R_g^2 = q^2(N_i b_i^2/6)$, where R_g is the radius of gyration, b_i is statistical segment length of polymer i, and q is the scattering length, $q = 4\pi \sin\theta/\lambda$. λ is the wavelength of the incident beam, and 2θ is the scattering angle.

Data from each miscible blend were fitted by eq 1 with χ and b_i as parameters obtained from a best fit[4] of the experimental data. For the fitting routine, an average value of b was assumed for the blend where the HPI and DPB polymers in each blend had the same statistical segment length (i.e., $b = b_1 = b_2$). χ as a function of T was obtained at nine different temperatures for each of 18 polymer−polymer blends. The effective χ values were plotted versus the reciprocal absolute temperature (T^{-1}) as in Figure 2. The χ/v_0 values and errors for the blends are given in Table 3.

Table 3. Polymer Blend SANS Data

x/y	0.07/0.09	0.07/0.09	0.07/0.09	0.07/0.26	0.07/0.26
ϕ_A/ϕ_B	0.72/0.28	0.52/0.48	0.32/0.68	0.52/0.48	0.32/0.68
T (K)	$\chi/v_0(\times10^5)$	$\chi/v_0(\times10^6)$	$\chi/v_0(\times10^5)$	$\chi/v_0(\times10^6)$	$\chi/v_0(\times10^5)$
308	−4.27(17)			−3.25(73)	1.02(9)
318	−3.83(20)	−0.07(103)	1.37(7)	−2.03(77)	1.27(8)
328	−3.93(17)	2.16(96)	1.53(8)	−0.39(75)	1.36(9)
338	−3.53(23)	2.76(104)	1.56(7)	2.18(81)	1.47(9)
348	−3.31(22)	4.61(83)	1.66(8)	3.41(64)	
353	−3.39(19)	5.08(86)			
363	−3.19(21)	6.47(96)	1.77(7)		
373		8.14(104)			

x/y	0.07/0.39	0.07/0.39	0.07/0.70	0.07/0.70	0.21/0.09
ϕ_A/ϕ_B	0.52/0.48	0.32/0.68	0.52/0.48	0.32/0.68	0.72/0.28
T (K)	$\chi/v_0(\times10^5)$	$\chi/v_0(\times10^5)$	$\chi/v_0(\times10^5)$	$\chi/v_0(\times10^5)$	$\chi/v_0(\times10^5)$
298			−4.99(7)	−4.60(13)	
308	−5.75(16)	−1.81(14)	−4.39(9)	−4.09(14)	3.67(5)
318	−5.65(17)	−1.71(12)	−3.89(9)	−3.69(12)	3.71(6)
328	−5.45(18)	−1.54(12)	−3.48(8)	−3.30(11)	
338	−5.35(18)	−1.52(11)	−3.03(7)	−2.88(11)	3.79(5)
348	−5.28(15)	−1.24(12)	−2.78(8)	−2.60(9)	3.81(5)
353		−1.26(13)	−2.52(9)	−2.46(10)	3.87(6)
363		1.21(14)	−2.33(9)	−2.24(9)	3.81(5)
373			−2.10(7)		3.84(5)

x/y	0.21/0.09	0.21/0.09	0.21/0.26	0.21/0.26	0.21/0.39
ϕ_A/ϕ_B	0.52/0.48	0.32/0.68	0.52/0.48	0.32/0.68	0.72/0.28
T (K)	$\chi/v_0(\times10^5)$	$\chi/v_0(\times10^5)$	$\chi/v_0(\times10^5)$	$\chi/v_0(\times10^5)$	$\chi/v_0(\times10^5)$
298			2.46(5)	1.72(6)	0.98(13)
308	3.77(4)		2.53(5)	1.83(7)	1.04(15)
318	3.80(4)	4.08(4)	2.61(5)	1.92(7)	1.08(12)
328	3.85(3)	4.12(4)	2.71(5)	2.05(5)	1.16(13)
338	3.89(4)	4.13(4)	2.77(5)	2.14(6)	1.22(11)
348	3.94(3)	4.17(4)	2.85(4)	2.23(6)	
353	3.98(3)	4.18(4)	2.89(5)		
363	3.99(3)	4.25(4)	2.93(4)	2.36(6)	
373	4.02(3)	4.29(3)		2.42(6)	

x/y	0.21/0.39	0.21/0.70	0.21/0.70	0.21/0.70	0.44/0.39
ϕ_A/ϕ_B	0.52/0.48	0.72/0.28	0.52/0.48	0.32/0.68	0.52/0.48
T (K)	$\chi/v_0(\times10^5)$	$\chi/v_0(\times10^5)$	$\chi/v_0(\times10^5)$	$\chi/v_0(\times10^5)$	$\chi/v_0(\times10^5)$
298	1.28(11)	−2.70(13)	−6.32(17)	−2.49(19)	3.76(15)
308	1.38(13)	−2.27(13)	−5.81(17)	−2.20(17)	3.73(12)
318	1.45(12)	−1.99(12)	−5.45(18)	−2.05(17)	3.72(12)
328	1.60(12)	−1.73(12)	−5.05(14)	−1.78(15)	3.62(13)
338	1.68(11)	−1.54(10)	−4.70(14)	−1.72(13)	3.52(11)
348	1.77(11)	−1.24(10)	−4.35(14)	−1.60(14)	
353			−4.29(12)	−1.44(13)	
363			−4.07(14)	−1.31(12)	

x/y	0.44/0.39	0.44/0.70	0.44/0.70	0.44/0.70
ϕ_A/ϕ_B	0.32/0.68	0.72/0.28	0.52/0.48	0.32/0.68
T (K)	$\chi/v_0(\times10^5)$	$\chi/v_0(\times10^5)$	$\chi/v_0(\times10^5)$	$\chi/v_0(\times10^5)$
298	1.04(23)	−9.36(22)	−4.02(19)	−6.97(40)
308	1.18(18)	−9.09(18)	−3.82(14)	
318	1.41(21)	−8.70(25)	−3.47(15)	−6.43(32)
328	1.49(21)		−3.31(13)	−6.32(32)
338	1.66(18)	−8.26(20)	−2.98(14)	−6.08(31)
348		−8.02(25)	−2.80(13)	−5.78(29)
353		−7.88(23)	−2.59(16)	
363			−2.53(15)	

The microstructure effects on χ for the HPI/DPB blends are shown in Figures 3 and 4 at $\phi_B = 0.5$. This composition ($\phi_B = 0.5$) was picked for the composition dependent χ because it was near the critical composition of the blend. The χ values are plotted versus T^{-1}. Figure 3 shows the effect of DPB microstructure and Figure 4 shows the effect of HPI microstructure on χ. The slopes of the χ values showed a linear relationship with T^{-1}, and the slopes were negative except for the blend HPI-44/DPB-39, which had a positive slope. Those blends with negative slopes have LCST behavior in spite of the differences in microstructures. From Figure 3, χ decreases as the 1,2 content of the DPB increases. From Figure 4, χ increases as the 3,4 content of the HPI increases, except for the HPI-7/DPB-70 blend curve which lies between that of HPI-21/DPB-70 and HPI-44/DPB-70. These results indicate that the blend becomes more miscible by increasing the 1,2 content of the DPB or by decreasing the 3,4 content of HPI. When the 1,2 content of the DPB and the 3,4 content of HPI are low, then the blend has an LCST and χ is positive.

The classical Flory−Huggins free energy of mixing can be expressed as

$$\Delta f = k_B T[(\phi_A/N_A v_A)\ln\phi_A + (\phi_B/N_A v_B)\ln\phi_B + \phi_A\phi_B\chi_F/v_0] \quad (4)$$

where Δf is the free energy of mixing.

In the SANS experiment, the interaction parameter, χ, is given by the well-known de Gennes formula[8] as shown in eq 1. At the zero scattering angle ($q = 0$), $S^{-1}(0)$ is equal to the second concentration derivative of the Flory−Huggins free energy equation and is given by

$$S^{-1}(0) = 1/(v_A N_A \phi_A) + 1/(v_B N_B \phi_B) - 2\chi/v_0 = \partial^2(\Delta f/kT)/\partial\phi_B{}^2 \quad (5)$$

χ, the effective interaction parameter from the SANS experiment, can then be used to determine χ_F, the temperature and composition dependent interaction parameter according to Sanchez[13] by combining eqs 4 and 5 to give

$$\chi = \chi_F + (\phi_B - \phi_A)\partial\chi_F/\partial\phi_B - {}^1/_2\phi_A\phi_B\partial^2\chi_F/\partial\phi_B{}^2 \quad (6)$$

χ_F has been shown to have compositional and temperature dependence which can be represented by an expansion function[14]

$$\chi_F = (1 + b\phi_B + e\phi_B{}^2)(a + c/T + k\ln T) \quad (7)$$

or similar to eqs 25 and 26 of ref 23. In this work, the higher order terms, $\phi_B{}^2$ and ln T, have been dropped because of the limited experimental data for each blend system to give the empirical formulae for χ_F as

$$\chi_F = (1 + b\phi_B)(a + c/T) \quad (8)$$

Then, from eqs 6 and 8, χ is given by

$$\chi = a(1 - b) + 3b\phi_B + c(1 - b)/T + 3bc\phi_B/T \quad (9)$$

The a, b, and c coefficients for temperature and compositional effects were determined from a least-squares calculation of eq 9 for each polymer−polymer blend system, and then χ_F was calculated from eq 8.

The next step was to take χ_F for each polymer−polymer blend system and transform these χ_F values into χ values dependent on microstructure. By using the equation for χ_F for two random copolymers, copolymer 1 (A_xB_{1-x}) and copolymer 2 (C_yD_{1-y}), given by ten Brinke and MacKnight,[9] χ_F is given by

$$\chi_F(x,y) = \chi_1 - \chi_2$$

$$\chi_1 = xy\chi_{AC} + (1 - x)y\chi_{BC} + x(1 - y)\chi_{AD} + (1 - x)(1 - y)\chi_{BD}$$

$$\chi_2 = x(1 - x)\chi_{AB} + y(1 - y)\chi_{CD} \quad (10)$$

where χ_1 and χ_2 are the intermolecular and intra-

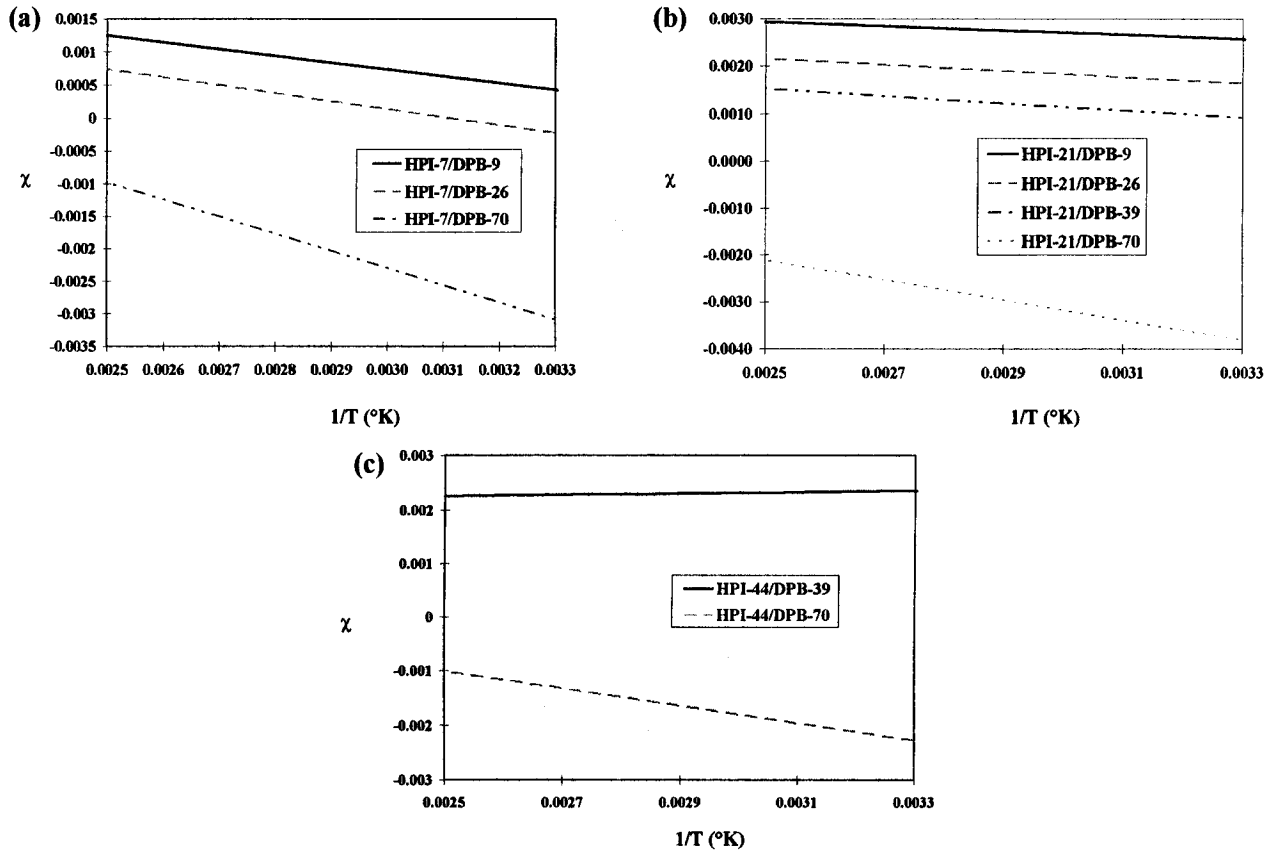

Figure 3. χ versus T^{-1} for (50/50) blends of (a) HPI-7 with DPB-9, DPB-26, and DPB-70; (b) HPI-21 with DPB-9, DPB-26, DPB-39, and DPB-70; (c) HPI-44 with DPB-39 and DPB-70. The number after HPI or DPB refers to 3,4 or 1,2 level, respectively.

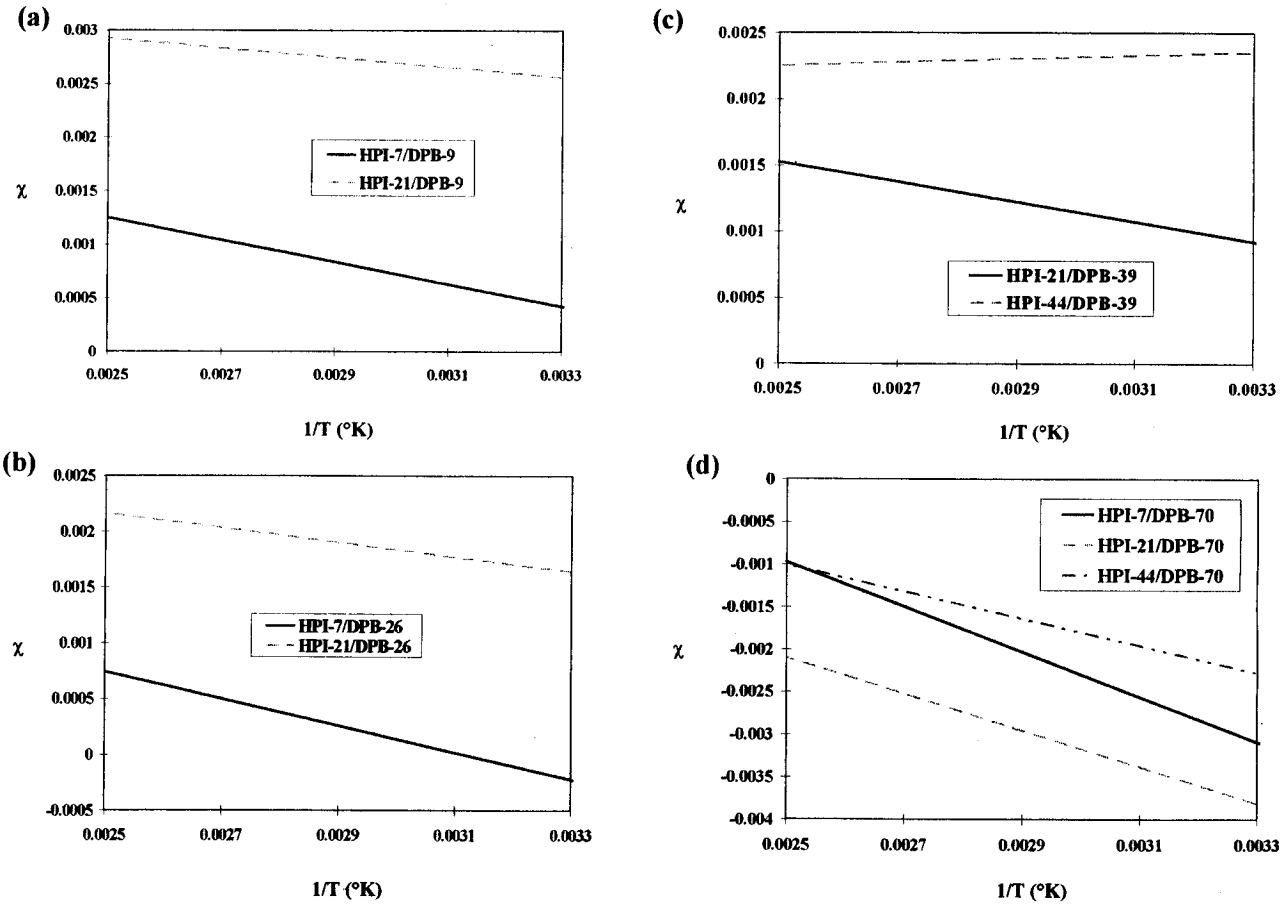

Figure 4. χ versus T^{-1} for (50/50) blends of (a) DPB-9 with HPI-7 and HPI-21; (b) DPB-26 with HPI-7 and HPI-21; (c) DPB-39 with HPI-21 and HPI-44; (d) DPB-70 with HPI-7, HPI-21, and HPI-44. The number after HPI or DPB refers to 3,4 or 1,2 level, respectively.

molecular interaction parameters, x and y are the copolymer compositions in volume fraction, and χ_{ij} (ij = A to D) is the segmental interaction parameter. Polybutadiene has three different segment units, i.e., the 1,2, cis-1,4, and trans-1,4 units. Polyisoprene has four different segment units, i.e., the 3,4, 1,2, cis-1,4, and trans-1,4 units. The 1,2 linkages for the polyisoprenes were small or zero and were not included in this work, although the 1,2 values of the polyisoprene were included in the total volume fraction. The cis-1,4 and trans-1,4 linkages are assumed to have the same χ_{ij} values. In eq 10, A is the 3,4 for HPI, B is the 1,4 for HPI, C is the 1,2 for DPB, and D is the 1,4 for DPB. A microstructural representation of the segmental interaction parameters for the HPI/DPB blends is shown in Figure 5. From the data in Table 1, the volume fractions of each segment for each polymer−polymer blend system were calculated and a set of simultaneous equations were made up for all $\chi_F(\phi_B,T)$ values from the SANS experiments. In this study, the eqs 10 for eight DPB/HPI blends with their individual $\chi_F(\phi_B,T)$ values were solved using matrix techniques. The inverted matrix was checked for nonsingularity by matrix multiplication with the original matrix. Standard errors were determined by taking the differences between the calculated and experimental results using statistical methods. The residual indices, R_i, for the coefficients of χ_F in eq 8 were calculated to be $R_a = 0.07$, $R_{ab} = 0.38$, $R_c = 0.09$, and $R_{cb} = 0.36$ by the equation:

$$R_i = \sum[|\chi_{oi} - \chi_{ci}|]/\sum|\chi_{oi}| \qquad (11)$$

where χ_{oi} is the ith observed interaction parameter coefficient and χ_{ci} is the ith calculated interaction parameter coefficient. The residual indices for the a and c coefficients from eq 8 for χ_F were within the experimental errors of SANS measurements. The residual indices for ab and cb coefficients from eq 8 were higher, possibly because only three and sometimes two compositions for a DPB/HPI blend were used.

We obtained the following segmental copolymer χ values for the eight simultaneous equations from eqs 10:

$$\chi_{AC} = -0.0151 + 0.0399\phi_B - 3.28/T - 3.44\phi_B/T \quad (12)$$
HPI(3,4)/DPB(1,2)

$$\chi_{BC} = 0.0116 - 0.0055\phi_B - 5.74/T + 1.73\phi_B/T$$
HPI(1,4)/DPB(1,2)

$$\chi_{AD} = -0.0025 + 0.0206\phi_B + 12.4/T - 19.2\phi_B/T$$
HPI(3,4)/DPB(1,4)

$$\chi_{BD} = 0.00399 + 0.0033\phi_B - 2.40/T + 1.09\phi_B/T$$
HPI(1,4)/DPB(1,4)

$$\chi_{AB} = -0.0138 + 0.0436\phi_B + 9/T - 21.4\phi_B/T$$
HPI(3,4)/HPI(1,4)

$$\chi_{CD} = 0.0132 - 0.0073\phi_B - 9.33/T + 7.61\phi_B/T$$
DPB(1,2)/DPB(1,4)

The six segmental interaction parameters as defined in Figure 5 are plotted in Figure 6 for $\phi_B = 0.5$. The χ_{AD} and χ_{AB} (interaction of 3,4 PI/1,4 PI and 3,4 PI/1,4 DPB, respectively) are positive over the temperature range of 20−100 °C. The other segmental interaction parameters are negative for the same temperature range. The

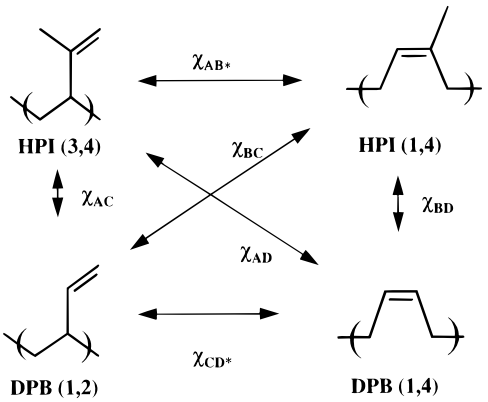

Figure 5. Microstructural representations of HPI and DPB with segmental interaction parameters.

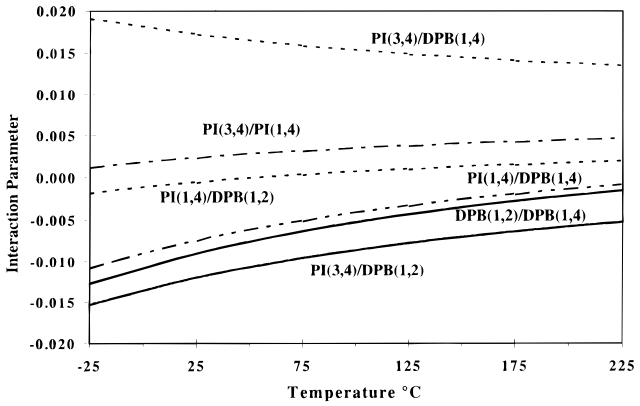

Figure 6. Segmental interaction parameters versus temperature.

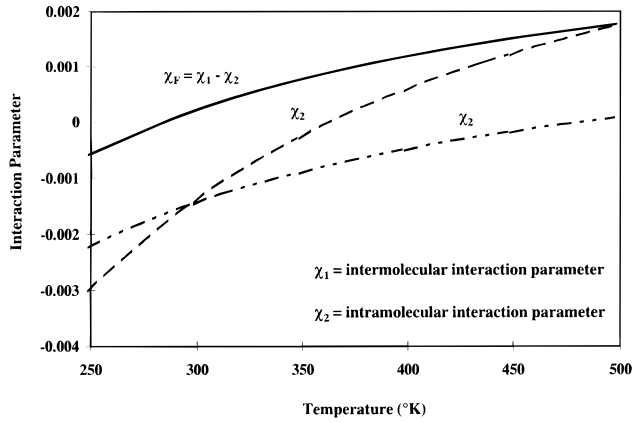

Figure 7. χ_F, χ_1, and χ_2 versus absolute temperature for 7% 3,4 HPI/24% 1,2 DPB blend (50/50).

results of Figure 6 indicate that, for HPI/DPB blends, χ_{AD}, the HPI(3,4)/DPB(1,4) parameter, has the strongest effect on miscibility.

The combined effect of the intermolecular interaction parameter, χ_1, as illustrated in Figure 7 for one blend, is a steady increase with temperature. This effect was determined for blends with microstructure ranges of PI 3,4 contents of 7−44% and DPB 1,2 contents of 9−70%. The intramolecular interaction shows a slight increase with an increase of temperature for all the ranges of microstructures examined in this work. χ_F also has a steady increase with temperature, as shown in Figure 7 for PI 3,4 of 7−21% and DPB 1,2 contents of 9−70%. A positive χ_F was determined when the PI 3,4 content

Table 4. Characterization Data for SALS Experiment

					microstructure (%)			
sample	T_g (°C)	$10^{-3}M_n$	$10^{-3}M_w$	M_w/M_n	3,4	cis-1,4	trans-1,4	1,2
HPI	-63	125	173	1.38	8	76	16	0
HBR	-85	165	168	1.02		30	46	24

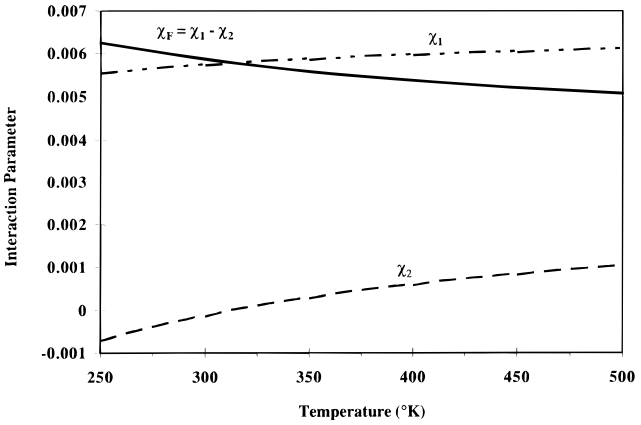

Figure 8. χ_F, χ_1, and χ_2 versus absolute temperature for 44% 3,4 HPI/9% 1,2 DPB blend (50/50).

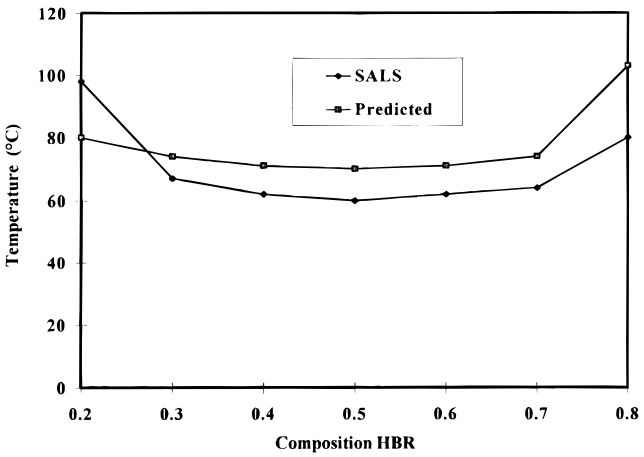

Figure 9. SALS and predicted cloud-point curves for a HPI/HBR blend.

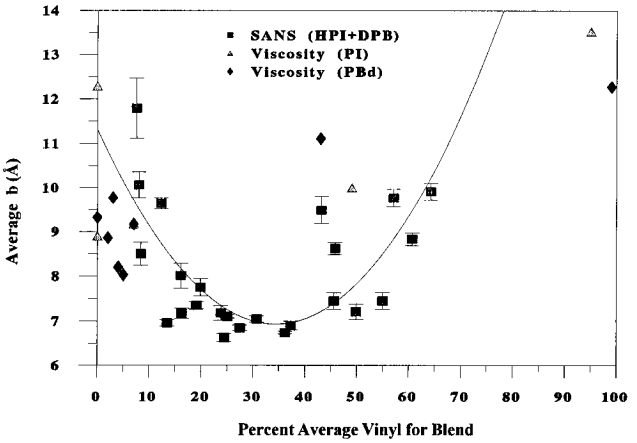

Figure 10. Statistical segment length (b) versus percent average vinyl for blend.

was 44% and the DPB 1,2 contents were 9−26%, as shown in Figure 8. When χ_{AD} has a significant contribution, χ_F will be positive and the blend will be immiscible.

The segmental interaction parameters were used to predict spinodal and cloud point curves. The spinodal points at a given temperature were obtained by letting the second derivative of the Flory−Huggins free energy eq 4 equal zero as given by:

$$\partial^2(\Delta f/kT)/\partial\phi_B{}^2 = 0 = 1/(v_A N_A \phi_A) + 1/(v_B N_B \phi_B) - 2\chi_F/v_0 \quad (13)$$

Since χ_F can be calculated from the six segmental interaction parameters of eqs 10 for a given microstructure, prudent choice of the 3,4 HPI content will give any desired LCST spinodal phase diagram using eq 13 and plotting T (K) versus ϕ_B. The cloud point phase diagram was obtained from BIOSYM software and described by Mumby[14,15] by fitting the minimum of the total free energy with equal chemical potential for the individual components in both phases.

A comparison of the theoretical (derived from the SANS data of binary blends of deuterated PBds and protonated PIs) and the experimental SALS data for a binary blend of protonated PBd and protonated PI was made by solution mixing two higher molecular weight polymers (Table 4). The predicted cloud-point curve and the experimental SALS data are shown in Figure 9. The agreement between the theoretical and the experimental data is good considering the experimental error of the SANS data and the fact that the isotopic effect between protonated and deuterated polybutadiene was not taken into consideration. We did not have deuterated polyisoprenes to blend with protonated polybutadiene (the opposite of that used in this work) as a blend system for SANS experiments. This type of blend system would allow us to determine the isotopic effect in polydiene blends. Several authors have described solutions of the excess free energies and phase separation[16−18] of deuterated and protonated polymers.

The average statistical segment length, b, as determined from the SANS experiments appears to be independent of temperature, but is dependent on the total vinyl level as shown in Figure 10. These b values showed a minimum value at 30−35% total vinyl for the binary blends examined by SANS. The error bars in Figure 10 are very small at this minimum value and suggest a real trend. Also, the statistical segment length calculated from viscosity data[19−22] of unperturbed end-to-end distance ($R_0^2 = nb^2$) are shown in Table 5 and also plotted in Figure 10.

Except for the 43% 1,2 polybutadiene value, these calculated statistical segment length values for homopolymers agree with average values of total vinyl of the binary blends determined using the random phase approximation from the SANS data as shown in Figure 10. For polydienes with 30−35% vinyl, one or both of the polymer chains must be more flexible in the chain backbone to result in a smaller b value.

A minimum statistical segment length has not been reported in the literature for polydienes with 30−35% vinyl. It would be interesting to check on this minimum with viscosity measurements for a polyisoprene and also a polybutadiene with 30−35% vinyl content.

Table 5. Calculated Statistical Segment Lengths

Polyisoprene				
cis-1,4	trans-1,4	3,4	*b* (Å)	ref
100	0	0	8.9	19
0	100	0	12.3	19
71	22	7	9.2	21
25	26	49	10.0	20
3	2	95	13.5	20
Polybutadiene				
cis-1,4	trans-1,4	1,2	*b* (Å)	ref
100	0	0	9.3	19
98	0	2	8.9	19
95	1	4	8.2	19
92	3	5	8.0	19
36	57	7	9.2	21
17	40	43	11.1	20
1		99	12.3	22
0	97	3	9.8	19

Conclusions

The HPI/DPB system has been modeled to determine phase behavior of known molecular weights, compositions, and microstructures. The interaction parameter, χ_F, for HPI/DPB blends increases with temperature for microstructures of 3,4 HPI content of 7−44% and 1,2 DPB contents of 39−70%. The interaction parameter, χ_F, for HPI/DPB blends decreases with temperature for microstructures of 3,4 HPI content of 44% and 1,2 DPB contents of 9−26%. The 3,4 microstructure of HPI is a strong controlling factor in the phase behavior of the HPI/DPB blend system. The 3,4 isomeric group is immiscible with 1,4 butadiene groups and miscible with the 1,2 butadiene group over a wide temperature range.

A minimum statistical segment length of 7 Å was determined from the SANS data for polymer−polymer blends with total vinyl of 30−35%.

Recommendations

A SANS experiment using deuterated polyisoprene with protonated polybutadiene (the opposite of that studied in this work) as a blend system would answer the question about the isotopic effect in polydiene blends when one polymer is deuterated, since this would give interaction parameters for all protonated PI/PBd blends by combining the two studies.

Acknowledgment. The authors express sincere thanks to W. Hsu and A. F. Halasa for synthesis of the polymers, to J. Koberstein, S. J. Walters, M. R. Ambler, and D. B. Trowbridge for helpful discussions, to H. Yoon for his help with the SANS experiments, and to J. Visintainer, R. C. Hirst, N. L. Dotson, and J. M. Massie for characterization of polymers.

References and Notes

(1) Sakurai, S.; Jinnai, H.; Hasegawa; H.; Hashimoto, T.; Han, C. *Macromolecules* **1991**, *24*, 4839.
(2) Hasegawa, H.; Sakurai, S.; Takenaka, M.; Hashimoto, T.; Han, C. *Macromolecules* **1991**, *24*, 1813.
(3) Sakurai, S.;Isumitani, T.; Hasibawa, H.; Hashimoto, T.; Han, C. *Macromolecules* **1991**, *24*, 4844.
(4) Shibayama, M.; Yang, H.; Stein, R.; Han, C. *Macromolecules* **1985**, *18*, 2179.
(5) Sakurai, S.; Hasegawa, H.; Hashimoto, T.; Hargis, I.; Aggarwal, S.; Han, C. *Macromolecules* **1990**, *23*, 451.
(6) Bates, F. S.; Wignal, G. D. *Phys. Rev. Lett*. **1986**, *57*, 1429.
(7) Jinnai, H.; Hasegawa, H.; Hashimoto, T.; Han, C. *J. Chem. Phys*. **1993**, *99*, 4845.
(8) de Gennes, P. G. *Scaling Concepts in Polymer Physics*; Cornell University Press: Ithaca, New York, 1979.
(9) ten Brinke, G.; Karasz, F.; MacKnight, W. *Macromolecules* **1983**, *16*, 1827.
(10) Paul, D.; Barlow, J. *Polymer* **1984**, *25*, 487.
(11) Glinka, C. J.; Rowe, J. M.; LaRock, J. G. *J. Appl. Crystallogr*. **1986**, *19*, 427.
(12) Walters, S. J.; Bell, R. S. Private communication.
(13) Sanchez, I. C. *Polymer* **1989**, *30*, 471.
(14) Qian, C.; Mumby, S. J.; Eichinger, B. E. *Macromolecules* **1991**, *24*, 1655.
(15) Mumby, S. J.; Qian, C.; Eichinger, B. E. *Polymer* **1992**, *33*, 5105.
(16) Singh, R. R; Van Hook, W. A. *Macromolecules* **1987**, *20*, 1855.
(17) Cifra, P.; Karasz, F. E.; MacKnight, W. J. *Macromolecules* **1988**, *21*, 446.
(18) Curro, J. G.; Schweizer, K. S. *J. Chem. Phys.* **1988**, *88*, 1988.
(19) Brandrup J.; Immergut, E. H. *Polymer Handbook*; Wiley: New York, 1975; IV-34.
(20) Mays, J.; Hadjichristidis, N.; Fetters, L. J. *Macromolecules* **1984**, *17*, 2723.
(21) Hadjichristidis, N.; Zhongde, X.; Fetters, L. J. *J. Polym. Sci.* **1982**, *20*, 743.
(22) Zhongde, X.; Hadjichristidis, N.; Carella, J. M.; Fetters, L. J. *Macromolecules* **1983**, *16*, 925.
(23) Han, C. C.; Bauer, B. J.; Clark, J. C.; Muroga, Y.; Matsushita, Y.; Okada, M.; Qui, T.; Chang, T.; Sanchez, I. C. *Polymer* **1988**, *29*, 2002.

MA9512465